

Lowering of ordering temperature for fct Fe–Pt in Fe/Pt multilayers

Yasushi Endo,^{a)} Nobuaki Kikuchi, Osamu Kitakami, and Yutaka Shimada

Research Institute for Scientific Measurements, Tohoku University, 2-1-1 Katahita, Aoba-ku, Sendai 980-8577, Japan

We have explored magnetic properties and structural characteristics of Fe/Pt multilayers after annealing at various temperatures in order to clarify the growth process of the ordered Fe–Pt phase in the Fe/Pt multilayer structures. It is found that rapid diffusion at Fe/Pt interface occurs at temperatures 275–325 °C and the multilayer structure directly transforms to the ordered (fct) phase when Fe and Pt layer thickness is almost equal. The ordering parameter S is evaluated to be 0.50–0.65 after annealing at 300–325 °C, and then is significantly enhanced to ~ 1.00 with increasing annealing temperatures. By comparing the thermal processes of these different multilayer structures, it is found that the rapid formation of the fct phase in the multilayers with Fe/Pt $\cong 1$ is due to relatively rapid diffusion at the interface. © 2001 American Institute of Physics. [DOI: 10.1063/1.1357150]

In the rapid development of the high-density magnetic recording media, the low noise and high thermal stability are needed with the reduction of the grain size. Recently, the equiatomic Co–Pt, Fe–Pd, and Fe–Pt alloy thin films have attracted much attention owing to very high magnetic anisotropies. In particular, the fct Fe–Pt alloy possess the highest magnetic anisotropy of $K_u \sim 7 \times 10^7$ erg/cc (Ref. 1) among these materials. The origin of the high magnetic anisotropy of this alloy is the ordered (fct) phase. However, the growth temperature of the fct phase in the granular Fe–Pt:SiO₂ films^{2,3} and the sputter deposited Fe–Pt films^{4,5} is higher than 500 °C except for the molecular beam epitaxy films.⁶ On the other hand, it was reported that this growth temperature in the multilayered Fe/Pt films is much lower than the others,⁷ although the details of the ordering process in the multilayered Fe/Pt films have not been clarified.^{7,8}

In this article, we investigate the magnetic properties and structural characteristics of as-prepared and annealed Fe/Pt multilayers, and the thermal process of transformation from the multilayer structure to a fct ordered single layer film is studied in detail.

Fe/Pt multilayers were grown on quartz substrates at ambient temperature in a dc magnetron sputtering system, with a base pressure less than 6.0×10^{-7} Torr and an argon gas pressure of 3 mTorr. The deposition rate of Fe and Pt layer was 0.95–1.15 and 0.90–1.10 Å/s, respectively. The multilayers were grown with the Fe layer thickness t_{Fe} fixed at 25 Å and the nominal Pt layer thickness t_{Pt} varied from 5–50 Å, with ten bilayers. The as-prepared samples were subjected to vacuum annealing at temperature (T_a) in the range of 200–500 °C for 1 h, in a vacuum higher than 1×10^{-6} Torr. The periodic and crystallographic structure of Fe/Pt multilayers were characterized by low-angle, high-angle, and 2θ -scan x-ray diffractions (XRD) using CuK α radiation. The superlattice period (Λ) were evaluated by the kinematical Bragg's law $\Lambda = l\lambda/2 \sin \theta$ for the l -th order reflection, here λ is the

x-ray wavelength and θ is the observed diffraction angle. Since the lower order reflection is seriously influenced by the refraction effect, we improved precision evaluating the periods for larger l by analyzing all detected Bragg reflections.⁹ The film compositions were determined by electron probe microanalysis (EPMA). Magnetic properties at room temperature were measured by a vibrating sample magnetometer.

Figure 1 shows annealing temperature (T_a) dependence of coercivity (H_c) on the Pt layer thickness (t_{Pt}) for [Fe(25 Å)/Pt(t_{Pt} Å)]₁₀ multilayers. As shown in Fig. 1, H_c for all t_{Pt} is almost null at $T_a < 300$ °C. At $T_a \geq 300$ °C, H_c for $15 \text{ Å} \leq t_{\text{Pt}} < 40 \text{ Å}$ remarkably increases with increasing annealing temperature. In particular, H_c for $t_{\text{Pt}} = 25 \text{ Å}$ shows the maximum value in this range of Pt layer thickness. Meanwhile, H_c for $t_{\text{Pt}} < 15 \text{ Å}$ remains low, and H_c for $t_{\text{Pt}} \geq 40 \text{ Å}$ slightly increases up to 1–2 kOe by annealing over $T_a = 350$ °C. Thus, the thermal change of H_c is found to be sensitive to Pt layer thickness. So, we minutely investigated

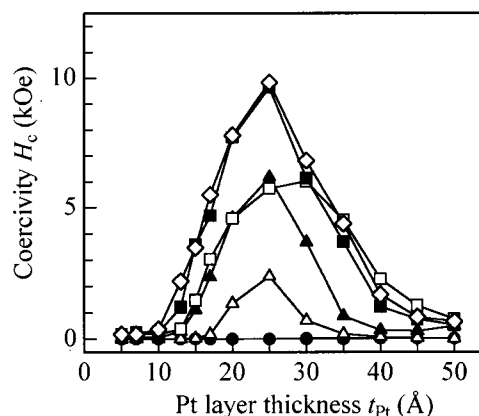


FIG. 1. Annealing temperature (T_a) dependence of coercivity (H_c) on the Pt layer thickness (t_{Pt}) for [Fe(25 Å)/Pt(t_{Pt} Å)]₁₀ multilayers. The external field for the measurement is in the sample plane. The marks (○), (●), (△), (▲), (□), (■), and (◇), respectively, are for as-prepared samples, annealed at $T_a = 200$ °C, 300 °C, 350 °C, 400 °C, 450 °C, and 500 °C.

^{a)} Author to whom all correspondence should be addressed; electronic mail: endo@rism.tohoku.ac.jp

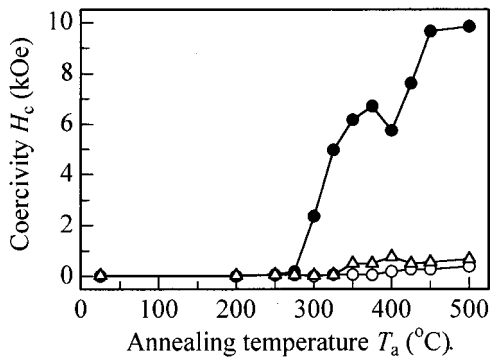


FIG. 2. Coercivity for $t_{\text{Pt}}=10, 25,$ and 50 \AA as a function of annealing temperature (T_a). The external field is induced in the sample plane. The marks (○), (●), and (△) are for $t_{\text{Pt}}=10, 25,$ and 50 \AA , respectively.

H_c for $t_{\text{Pt}}=10, 25,$ and 50 \AA at the various annealing temperatures. As seen in Fig. 2, H_c for $t_{\text{Pt}}=25 \text{ \AA}$ is significantly enhanced from 0.2 to ~ 10 kOe after annealed $275^\circ\text{C} \leq T_a < 425^\circ\text{C}$. This rapid change should be attributed to formation of the ordered (fct) phase at the Fe/Pt interface, as will mentioned later. As compared with the single layer Fe–Pt films^{4,5} and the granular FePt:SiO₂ films,^{2,3} the ordering temperature is reduced by nearly 300°C . According to M – H loops after annealing at $T_a=300^\circ\text{C}$ (Fig. 3), the easy axis of the magnetization for $t_{\text{Pt}}=25 \text{ \AA}$ mainly lies in the sample plane, and this feature holds for all annealing temperatures. On the other hand, H_c for $t_{\text{Pt}}=50 \text{ \AA}$ starts to increase at $T_a=350^\circ\text{C}$, but it increases very slowly with annealing temperatures. Moreover, H_c for $t_{\text{Pt}}=10 \text{ \AA}$ is very low and almost independent of T_a . This suggests that the different Fe–Pt phases such as Fe₃Pt and FePt₃ are formed at the Fe/Pt interface when the ratio of Fe and Pt layer thickness $t_{\text{Fe}}/t_{\text{Pt}}$ deviates from one.

In order to study formation of the different Fe–Pt phases depending on Fe and Pt layer thickness, we carefully explored the structural change for annealed $[\text{Fe}(25 \text{ \AA})/\text{Pt}(t_{\text{Pt}} \text{ \AA})]_{10}$ ($t_{\text{Pt}}=10, 25,$ and 50 \AA) multilayers. The low-, high-angle, and 2θ -scan XRD patterns of as-prepared and annealed $[\text{Fe}(25 \text{ \AA})/\text{Pt}(25 \text{ \AA})]_{10}$ multilayers are shown in Fig. 4. This sample possesses well defined multilayer structures at $T_a < 300^\circ\text{C}$. At $T_a=300^\circ\text{C}$, the second and third order reflections disappear in the low-angle

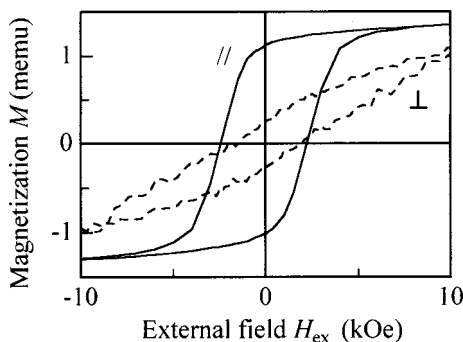


FIG. 3. M – H loops for $[\text{Fe}(25 \text{ \AA})/\text{Pt}(25 \text{ \AA})]_{10}$ multilayer at $T_a=300^\circ\text{C}$. The solid line and broken line indicate the external field in the sample plane and perpendicular to the sample plane.

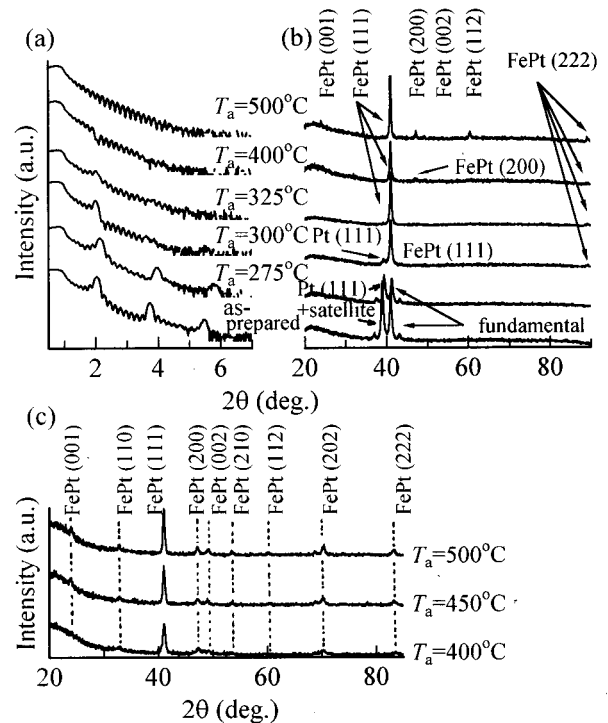


FIG. 4. The low-angle (a), high-angle (b), and 2θ -scan XRD patterns for $[\text{Fe}(25 \text{ \AA})/\text{Pt}(25 \text{ \AA})]_{10}$ multilayer at various annealing temperatures.

XRD patterns [Fig. 4(a)]. And also, in the high-angle XRD patterns [Fig. 4(b)], the satellite peak by multilayer structure is completely lost and Pt(111) peak is very weak at $T_a=300^\circ\text{C}$, and then the ordered (fct) FePt(111) and (222) peak can be observed at $2\theta=41.1^\circ$ and 89° , respectively. These results indicate that the rapid diffusion at Fe/Pt interface occurs at lower temperatures and the multilayer structure directly transforms to the fct FePt phase. Furthermore, residuals of Fe and Pt seem negligible after annealing above 300°C . In order to investigate the growth degree of the fct phase for $t_{\text{Pt}}=25 \text{ \AA}$ in more detail, the ordering parameter S was evaluated as follows. In the ordered (fct) phase, there are two kinds of atomic sites which are designated as α and β . For the ideal stoichiometric composition of Fe_{0.50}Pt_{0.50} and the perfect long-range ordering, the α sites are all occupied by Fe atoms and β sites by Pt atoms. The ordering parameter S is defined as¹⁰

$$S = 2(\gamma_\alpha - x_{\text{Fe}}) = 2(\gamma_\beta - x_{\text{Pt}}), \quad (1)$$

where x_{Fe} and x_{Pt} are atomic fractions of Fe and Pt, and γ_α and γ_β the fraction of α and β sites occupied by the right atom, respectively. $S=1$ means that the phase is fully ordered if the composition is stoichiometric and $\gamma_\alpha = \gamma_\beta = 1$; Deviation of either composition from 0.5 or γ_{Fe} (or γ_{Pt}) from 1 results in $S < 1$. For the sample with $t_{\text{Pt}}=25 \text{ \AA}$, the composition was determined to be Fe:Pt=0.52:0.48 by EPMA,¹¹ and so, S should be 0.94 from Eq. (1) if the sample is perfectly ordered. The fully ordered phase was confirmed at $T_a \geq 450^\circ\text{C}$ by the high-angle XRD [Fig. 4(b)]. At $300^\circ\text{C} \leq T_a \leq 425^\circ\text{C}$, the superstructure peaks such as (001), (110), and (002) etc. are not detectable in the high-angle XRD patterns, as seen in Fig. 4(b). However, for the sample at

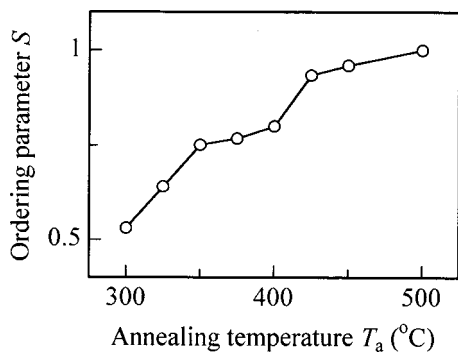


FIG. 5. Annealing temperature (T_a) dependence of the ordering parameter (S) for $[\text{Fe}(25 \text{ \AA})/\text{Pt}(25 \text{ \AA})]_{10}$ multilayer.

$300 \text{ }^\circ\text{C} \leq T_a \leq 425 \text{ }^\circ\text{C}$, the partially ordered phase should be formed because the coercivity is remarkably enhanced as described above. For the partially ordered phase, the ordering parameter S can be determined from the axial ratio c/a , and is in good agreement with the S values determined from the x-ray intensity measurements. The ordering parameter S is given by¹²

$$S^2 = \frac{1 - (c/a)}{1 - (c/a)_{S_f}} \quad (2)$$

where $(c/a)_{S_f}$ is the axial ratio for the fully ordered phase (S_f), and (c/a) is for the partially ordered phase. $S=1$ in Eq. (2) means the fully ordered phase regardless of composition deviation, and is different from that in Eq. (1). In Fig. 4(c), the several superstructure peaks can be observed in 2θ -scan XRD patterns, and so, (c/a) of the sample after annealing at $T_a \leq 425 \text{ }^\circ\text{C}$ can be evaluated from the superstructure and fundamental peaks in these patterns. Moreover, $(c/a)_{S_f}$ was determined to be 0.961 from the position of (110) and (002) peaks from the fully ordered phase after annealing at $T_a = 500 \text{ }^\circ\text{C}$. Accordingly, the ordering parameter S obtained by Eq. (2) using 2θ -scan XRD patterns is shown in Fig. 5. S is significantly enhanced from 0.50 to 0.90 with increasing annealing temperatures up to $425 \text{ }^\circ\text{C}$. After annealing over $450 \text{ }^\circ\text{C}$, S is almost 1.00 suggesting the fully ordered phase. This thermal change of S coincides with that of H_c , and supports the inference that the fct Fe–Pt phase is directly formed via the rapid diffusion at the Fe/Pt interface when Fe and Pt layer thickness is almost equal.

On the other hand, the different phases such as Fe_3Pt and FePt_3 crystalline phase are formed for $t_{\text{Pt}} = 10$ and 50 \AA , as seen in Fig. 6. In contrast to $t_{\text{Pt}} = 25 \text{ \AA}$, these multilayer structures are stable up to near $T_a = 400 \text{ }^\circ\text{C}$. In the case of $t_{\text{Pt}} = 10 \text{ \AA}$, $\text{Fe}_3\text{Pt}(200)$ peak is observed at $2\theta = 48.5^\circ$. And also, for $t_{\text{Pt}} = 50 \text{ \AA}$, $\text{FePt}_3(200)$ and (311) peaks are observed at $2\theta = 47.0^\circ$ and 82.7° , respectively. This indicates that the different phases, such as Fe_3Pt and FePt_3 phases, are formed from the multilayer structure when the ratio of Fe and Pt layer thickness deviates from one.

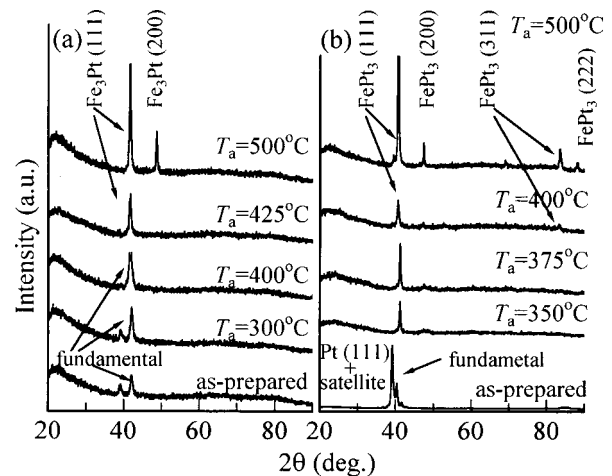


FIG. 6. The high-angle XRD patterns of (a) $[\text{Fe}(25 \text{ \AA})/\text{Pt}(10 \text{ \AA})]_{10}$ and (b) $[\text{Fe}(25 \text{ \AA})/\text{Pt}(50 \text{ \AA})]_{10}$ multilayers at various annealing temperatures.

In summary, from the relation between the magnetic properties and the structural characteristics for as-prepared and annealed Fe/Pt multilayers, it is found that the ordering temperature is drastically reduced and the ordering parameter S is evaluated to be 0.50–0.65 after annealing at 300 – $325 \text{ }^\circ\text{C}$ when Fe and Pt layer thickness is equal. This appreciable reduction is correlated with rapid diffusion at the interface of Fe/Pt, and subsequently, the faster corruption of the multilayer structure. On the other hand, the different Fe–Pt crystalline phases such as Fe_3Pt and FePt_3 phase are formed when the thickness ratio of Fe/Pt deviates from one after annealing by relatively high temperature annealing.

One of the authors (Y.E.) is Research Fellow of the Japan Society for the Promotion of Science. The authors are greatly indebted to Y. Sato for performing EPMA analysis. The 2θ -scan XRD measurements were performed at the Laboratory for Developmental Research of Advanced Materials, the Institute for Material Research, Tohoku University. This work is supported by Research for the Future Program of Japan Society for the Promotion of Science under Grant No. 97R14701.

¹O. A. Ovanov, L. V. Solina, and V. A. Demshina, *Phys. Met. Metallogr.* **35**, 81 (1973).

²C. P. Luo and D. J. Sellmyer, *Appl. Phys. Lett.* **75**, 3162 (1999).

³C. P. Luo, S. H. Liou, and D. J. Sellmyer, *J. Appl. Phys.* **87**, 6941 (2000).

⁴K. R. Coffey, M. A. Parker, and J. K. Howard, *IEEE Trans. Magn.* **31**, 2737 (1995).

⁵M. R. Visokay and R. Sinclair, *Appl. Phys. Lett.* **66**, 1692 (1995).

⁶A. Cellollada, D. Weller, J. Sticht, G. R. Harp, R. F. C. Farrow, R. Marks, R. Savoy, and J. C. Scott, *Phys. Rev. B* **50**, 3419 (1994).

⁷C. P. Luo and D. J. Sellmyer, *IEEE Trans. Magn.* **31**, 2764 (1995).

⁸T. C. Hufnagel, M. C. Kautzky, B. J. Daniels, and B. M. Clemens, *J. Appl. Phys.* **85**, 2609 (1999).

⁹Y. Fujii, *Metallic Superlattices*, edited by T. Shinjo and T. Takada (Elsevier, Amsterdam, 1987), p. 33.

¹⁰B. E. Warren, *X-ray Diffraction* (Dover, New York, 1990), pp. 208–210.

¹¹Y. Endo, N. Kikuchi, O. Kitakami, and Y. Shimada (submitted).

¹²B. W. Roberts, *Acta Metall.* **2**, 597 (1954).